Title
A platform for investigating immune checkpoint-mediated changes in metabolism

Author
Palaskas, Nicolaos Jay

Publication Date
2017

Peer reviewed|Thesis/dissertation

UNIVERSITY OF CALIFORNIA

Los Angeles

A platform for investigating immune checkpoint-mediated changes in metabolism

A dissertation submitted in partial satisfaction of the

requirements for the degree Doctor of Philosophy in Molecular, Cellular, and Integrative Physiology

by

Nicolaos Jay Palaskas

2017

ABSTRACT OF THE DISSERTATION

A platform for investigating immune checkpoint-mediated changes in metabolism

by

Nicolaos Jay Palaskas

Doctor of Philosophy in Molecular, Cellular, and Integrative Physiology

University of California, Los Angeles, 2017

Professor Thomas G. Graeber, Chair

There is a growing interest in metabolomic profiling of immune cells, as there is accumulating evidence that metabolism influences immune cell function and fate decisions. The non-adherent nature of these cells presents certain challenges not factored into extraction protocols developed for adherent cells. Here, we present a method developed for metabolite extraction from human T-cells that emphasizes simplicity and economy. We apply this method to profile the metabolic changes effected by in-vitro programmed cell death 1 receptor (PDCD1/PD-1) immune checkpoint engagement by liquid chromatography and mass spectrometry. We demonstrate that we can efficiently confirm the known reduction in aerobic glycolysis and glutaminolysis that accompanies PD-1 signaling and extend this by showing a block in de novo nucleoside phosphate biosynthesis.

The dissertation of Nicolaos Jay Palaskas is approved.

Dimitrios Iliopoulos

Alexander Hoffman

Heather R. Christofk

Thomas G. Graeber, Committee Chair

University of California, Los Angeles

2017

Table of Contents

List of Figures

List of Tables

Acknowledgments

N.J.P. received financial support from the Division of Hematology-Oncology of the David Geffen School of Medicine at UCLA and from the Ruth L. Kirschstein National Research Service Award 5T32CA009297-30 (T32), Academic Training in Medical Oncology.

Thanks to: The Antoni Ribas lab for resource support, Daniel Shin and Cristina Puig Saus for assistance with flow cytometry and F5 T-cells. The staff of the UCLA Metabolomics Shared Resource, undergraduate students Jake Garcia and Roksana Shirazi for their help in generating data.

Vita

Education

Ph.D., Molecular Cellular and Integrative Physiology, UCLA (Expected)	2017
M.D., Aristotle University of Thessaloniki, Greece	2004

Postdoctoral Training

Hematology/Oncology Fellowship, UCLA, Los Angeles, CA	2012-2017
Postdoctoral Fellow/Scholar, Human Oncology and Pathogenesis Program, Memorial Sloan-Kettering Cancer Center, New York, NY	2011-2012
Internal Medicine Residency, St Elizabeth's Medical Center, Boston, MA	2008-2011
Postdoctoral Fellow/Scholar, Molecular and Medical Pharmacology, UCLA, Los Angeles, CA	2005-2008

Other Positions and Employment

Hospitalist, Spaulding Hospital Cambridge, Boston MA	2011-2012

Grants and Fellowships

Ruth L. Kirschstein National Research Service Award 5T32CA009297-30 (T32), Academic Training in Medical Oncology	2013-2014
Cancer Education and Career Development Program (R25T) Scholars in Oncologic Molecular Imaging, National Cancer Institute	2006-2008

Awards

TUFTS University School of Medicine Accomplished Teacher in Medicine	2010-2011

Advising and Mentoring

Jacob Garcia; Molecular, Cell, and Developmental Biology; Undergraduate Research Clerkship	2015-2016

Certification and Licensure

Diplomate, Internal Medicine ABIM	2011
Diplomate, Hematology ABIM	2016
Diplomate, Oncology ABIM	2016
California State Medical License	2010-
Massachusetts State Medical License	Inactive

Publications

Peer-reviewed publications

1. Graham NA, Minasyan A, Lomova A, Cass A, Balanis NG, Friedman M, Chan S, Zhao S, Delgado A, Go J, Beck L, Hurtz C, Ng C, Qiao R, Ten Hoeve J, **Palaskas N**, et al. Recurrent patterns of DNA copy number alterations in tumors reflect metabolic selection pressures. *Mol Syst Biol*. 2017 Feb 15;13(2):914. doi: 10.15252/msb.20167159. PubMed PMID: 28202506; PubMed Central PMCID: PMC5327725.

2. Shin DS, Zaretsky JM, Escuin-Ordinas H, Garcia-Diaz A, Hu-Lieskovan S, Kalbasi A, Grasso CS, Hugo W, Sandoval S, Torrejon DY, **Palaskas N**, et al. Primary Resistance to PD-1 Blockade Mediated by JAK1/2 Mutations. *Cancer Discov*. 2017 Feb;7(2):188-201. doi: 10.1158/2159-8290.CD-16-1223. Epub 2016 Nov 30. PubMed PMID: 27903500; PubMed Central PMCID: PMC5296316.

3. Rohle D*, Popovici-Muller J*, **Palaskas N***, Turcan S*, et al. An inhibitor of mutant IDH1 delays growth and promotes differentiation of glioma cells. *Science*. 2013 May 3;340(6132):626-30. PMID: 23558169; PMCID: PMC3985613.

4. **Palaskas N**, et al. 18F-fluorodeoxy-glucose positron emission tomography marks MYC-overexpressing human basal-like breast cancers. *Cancer Res*. 2011 Aug 1;71(15):5164-74. PMID: 21646475; PMCID: PMC3148325.

5. Vivanco I, Rohle D, Versele M, Iwanami A, Kuga D, Oldrini B, Tanaka K, Dang J, Kubek S, **Palaskas N**, et al. The phosphatase and tensin homolog regulates epidermal growth factor receptor (EGFR) inhibitor response by targeting EGFR for degradation. *Proc Natl Acad Sci U S A*. 2010 Apr 6;107(14):6459-64. PMID: 20308550; PMCID: PMC2851999.

6. Vivanco I, **Palaskas N**, et al. Identification of the JNK signaling pathway as a functional target of the tumor suppressor PTEN. *Cancer Cell*. 2007 Jun;11(6):555-69. PubMed PMID: 17560336.

* Equal contribution

Invited Presentations

Gene expression profiling and PET imaging. Joint Science Club Meeting of the Human Oncology and Pathogenesis Program and the Department of Cancer Biology and Genetics, Memorial Sloan-Kettering Cancer Center, 1275 York Avenue, New York, NY 10065	03/14/2008

CHAPTER 1

Introduction

Immune therapies for cancer have met unprecedented success in the recent years[1]. T-cells are central to anti-tumor immune surveillance[2] and several approaches with varying degrees of success have been used to stimulate them to attack tumors. These methods include vaccines[3], bispecific antibodies (BiTEs)[4,5], and adoptive cell transfer (ACT) with innate or engineered tumor recognition surface receptors[6–8].

Immune checkpoint blockade targeting Programmed Cell Death 1 (PDCD1/PD-1) and its ligand CD274 molecule (more commonly referred to as PD-L1) has captured the lion's share of attention due to the long term responses in the metastatic setting with limited toxicities[9,10]. T-cells can often be found at the tumor margin and infiltrate and proliferate within the tumor upon successful immune checkpoint blockade[11]. A critical shortcoming, however, is that some patients display de novo refractoriness, despite high mutational burden and predicted immunogenicity[12]. Often, the tumors of these patients will either not have inhibitory ligand expression, as measured by immunohistochemical methods, or will not have an appreciable immune infiltrate at the tumor margin[11]. This suggests 1) other immune suppression mechanisms or 2) a more profound immune exhaustion, which may even require adoptive T-cell transfer (ACT) for immune checkpoint blockade to be effective. As the experience with checkpoint inhibitor therapy matures, cases of acquired resistance are a growing clinical challenge[12,13]. Furthermore, recent data suggests that PD-1 signaling must be targeted with caution, as PD-1 is necessary to prevent T-cell terminal differentiation and exhaustion in a murine model of chronic

viral infection[14]. Thus, a better understanding of T-cell function and fate decisions in these contexts is needed.

There is mounting evidence for the regulatory role of metabolism in T-cell effector function and determination of cell fate, giving rise to the concept of metabolic checkpoints in T-cells[15]. It is known that T-cell metabolism is highly regulated, with a requirement for constant cytokine signaling to maintain homeostasis and basal proliferation. Upon activation the cells undergo drastic metabolic reprogramming. They switch metabolic prominence from full catabolism of glucose via the Krebs cycle and oxidative phosphorylation (OXPHOS) to aerobic glycolysis, resulting in high levels of lactate production and a redirection of glucose to the pentose phosphate shunt, very much akin to the Warburg effect in cancer. Immune checkpoint signaling can alter the capacity of the cells to fully maintain this metabolic program[16,17]. Beyond the common viewpoint of signaling regulating metabolic activity, there are recent examples of the direct effect of nutrient restriction on effector function, suggesting cancer can escape immune surveillance by out-competing effector cells for key nutrients[18–20], thus raising the potential for metabolism- and nutrient-based therapies.

By understanding the effect of metabolism on lymphocyte effector functions and fate decisions one can then seek ways to manipulate and direct those decisions to achieve more robust and long lasting immune-based therapies. Already, there are such proof of principle studies in the context of adoptive cell transfer in murine models[21–23]. Additionally, the similarities of the activated T-cell phenotype to cancer has led some to propose T-cell metabolic reprogramming as a model for the study of the Warburg phenomenon and carcinogenesis[24]. Yet, from a therapeutic standpoint, exposing the metabolic dissimilarities between cancer and immune metabolism is desirable, as

one would want to exploit such targets to inhibit tumor cells while promoting immune cell function.

Using unbiased methods to explore metabolic checkpoints in T-cells holds promise to uncover these targets. Mass spectrometry is an unbiased technology that has radically changed the field by providing the ability to do systems-level analyses of metabolism[25]. It has allowed for the discovery of new tumor-associated metabolites and changes in metabolic pathway fluxes that result from aberrant expression of normal proteins or cancer-related mutations. The production of the "oncometabolite" 2-hydroxyglutarate by mutant isocitrate dehydrogenase in gliomas and the increased production of nucleotides as a consequence of expression of the M2 isoform of the glycolytic enzyme pyruvate kinase (PKM2) are two notable examples[26,27].

Mass spectrometry has also been applied to gain insight into T-cell metabolism[17,28,29]. Nonetheless, currently there is no consensus regarding how to prepare non-adherent mammalian cell samples for metabolomics and even less guidance specifically for immune cells[30,31]. This may explain why two of the above cited studies required approximately 3 x 10^7 T-cells per replicate to achieve their observed results. Others are aspiring to perform single-cell metabolomics on *Aplysia californica* neurons[32], hinting that there may be room for improvement also for T-cells, provided the appropriate protocols and equipment. In any metabolomics assay, the samples must be prepared in a reproducible manner that maintains intracellular metabolite integrity. Hence, for T-cells the basic objectives are to rapidly quench metabolic activity and remove extracellular contaminating media metabolites by washing, before extracting the metabolites from the cells[30,31,33,34].

In light of the growing interest in immune cell metabolism, we undertook this study with the goal of developing an extraction protocol specifically suited for human T-cells. In some assays, sophisticated technologies and automation can help push the boundaries of low input and ease[32,35,36]. Our goal was to provide a simple and easily transferable protocol, while still improving economy in cellular input compared to previous studies[17,28]. Although the general approach in previous studies has been to achieve the highest yields of certain subsets of metabolites, we preferred to take a step beyond that and to set the bar at reproducing known T-cell biology to validate our method. Antigen-naïve T-cells are known to undergo drastic metabolic changes upon immune-challenge. They shift away from a basal, catabolic metabolism that relies primarily on oxidative phosphorylation, to aerobic glycolysis and glutaminolysis in order to meet their anabolic and effector function requirements[15,18,28,37]. There is also a growing appreciation of the role metabolism plays in T-cell fate and differentiation; with most knowledge centering around the balance between aerobic glycolysis, glutaminolysis and higher mTOR activity determining short-lived effector fates on one hand, and oxidative phosphorylation with consumption of alternative fuels such as fatty acids leading to regulatory cells and long-lived memory cells on the other[18,22,29,37,38]. It has been demonstrated that activating the PD-1 signaling axis downregulates aerobic glycolysis[16]. During the course of our study, it was published that PD-1 also reduces glutaminolysis and increases the reliance on fatty acid oxidation[17]. Given our interest in how T-cell metabolism relates to immune checkpoint inhibition therapy, we questioned whether through an optimized metabolomics protocol we could confirm and augment what is known about the metabolic reprogramming induced in human T-cells by PD-L1:PD-1 axis signaling.

CHAPTER 2

Development of a T-cell metabolite extraction protocol

Our goal was to develop a method that would balance easy transferability to other labs and reduced cellular input requirement, with the usual aims of rapid quenching of metabolism and elimination of contaminating extracellular metabolites. For the latter two objectives, rapid filtration solutions of different levels of sophistication have been proposed for prokaryotic and eukaryotic cells[35,36,39,40]. Early in our investigation we chose to evaluate a filter-based method originally applied to microbial extraction that did not require pumps and automation[40], but despite experimenting with several filter types and sizes we found filter clogging to be an issue. This limitation and reports of suboptimal recovery of metabolites from filters[30,41] led us to prioritize a centrifugation-based strategy.

Thus, we sought to find a quenching and washing solution that would maintain cell integrity for the duration of our customary centrifugation protocol (4 min at 500 x G-force). Some solutions used or formally tested in the past for metabolite extraction of non-adherent cells include phosphate buffered solution (PBS) with human and murine T-cells[17,28], 0.9% (w/v) NaCl[30] or 0.85% ammonium bicarbonate (AMBIC) in 60% methanol[33] with Chinese hamster ovary cells (CHO), 0.3% ammonium acetate and ammonium formate with the Jurkat T-cell leukemia cell line[31], and 5% mannitol with human leukemia cell lines[42]. Although very short exposure to deionized water (~2s) appears feasible in certain contexts with adherent cells[43], osmotic shock has been reported to result in leakage of solutes[44]. Methanol exposure also was reported to compromise cell membrane integrity and cause leakage[30,34,44]. We reasoned that microscopy could serve as a quick screening test to assess gross morphological changes with exposure to the

various wash solutions. As expected, gross changes were not observed with isotonic salt solutions or 5% mannitol (**Fig. 1a**), however 150 mM ammonium acetate caused significant swelling of the cells and 60% methanol/AMBIC solution distorted the cells upon contact (**Fig. 1a**). The drastic changes induced by the methanol/AMBIC solution and the poor metabolic profiling results reported by others[30,34] led us not to examine this approach further.

To determine whether the swelling seen with ammonium acetate would have a negative impact on metabolite measurements, we exposed spontaneously immortalized mouse embryonic fibroblasts (MEF) to ammonium acetate or NaCl wash solutions and removed the solutions immediately after one swirl in the tissue culture dish, after 20 seconds, or after 60 seconds, taking advantage of the adherent nature of these cells. Metabolite extraction was performed directly on the plate. Principal component analysis of 137 identified metabolites showed that the variability of biological replicate measurements increased as a function of time with the ammonium acetate wash (**Fig. 1b**). Loss of signal of the tricarboxylic acid cycle (TCA) metabolites has been suggested as a better indication of leakage than more highly charged phosphorylated metabolites[33]. We found most TCA metabolite signals were decreased at 60 s with the ammonium acetate wash (**Fig. 1c**), a much shorter time-point than our 4 min point required in a centrifugation protocol. On the contrary, the signal for citrate and aconitic acid was higher and increased as a function of time, as did the variability among replicates. The signal was more stable and consistent among replicates with the isotonic NaCl wash (**Fig. 1d**).

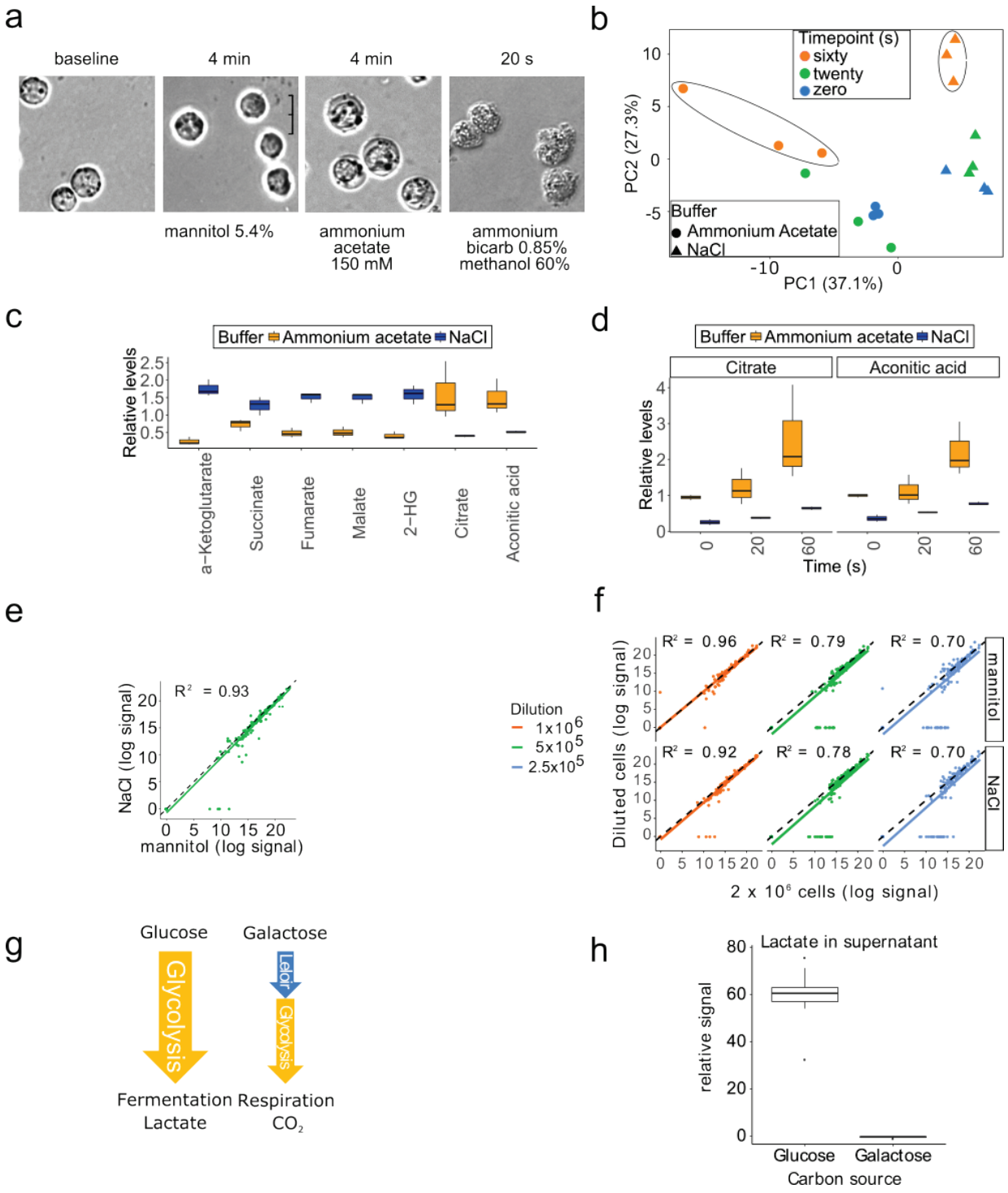

Figure 1. Meaningful metabolic changes can be profiled from immune cells with low cellular inputs using a mannitol wash solution.

(a) Light microscopy images show changes in cellular morphology with certain wash solutions. Jurkat cells were exposed to different wash solutions for the indicated time intervals. The ammonium acetate iso-osmotic wash buffer provides little tonicity and causes considerable

swelling of the cells. The ice-cold ammonium bicarbonate solution in 60% methanol causes cell changes on contact. In contrast, such changes are not noted with the mannitol solution. **(b)** Principal component analysis of 137 profiled metabolites demonstrates that the variance of intracellular metabolite measurements increases as a function of time when exposed to the ammonium acetate solution. Spontaneously immortalized 3T3 mouse embryonic fibroblasts were exposed to a 0.9% NaCl or 150 mM ammonium acetate solutions for the indicated times. The ellipses were added for emphasis. **(c)** The levels of the intracellular tricarboxylic acid cycle intermediates alpha-ketoglutarate, succinate, fumarate, and malate decrease with the 60 second ammonium acetate buffer exposure, suggestive of leakage from 3T3 cells. **(d)** Levels of citrate and aconitic acid are relatively stable with the NaCl wash solution and thus not indicative of leakage. **(e)** Correlation of profiled metabolites between mannitol and NaCl wash solutions. Triplicates of 2 x 10^6 Jurkat cells per condition. **(f)** Correlation of metabolite measurements of two-fold serially diluted samples. Values are corrected for the dilution factor. The dashed lines represent a perfect correlation. The solid colored lines are the best fit lines of the data. **(g)** Schematic displaying the reduced flux of galactose derived intermediates ending with complete oxidation to CO_2 compared to high glycolytic flux with glucose and production of lactate. **(h)** Supernatant lactate levels of activated primary human T-cells in glucose- or galactose-containing culture medium. Displayed are the summary results of three experiments, sampled from three replicate wells per condition (n = 9 vs. 9).

We decided to consider further only isotonic solutions and compared NaCl to mannitol using 2 x 10^6 Jurkat cells, as a model of suspension cells and human primary T-cells. Measurements were highly correlated between samples processed with each wash buffer, with mannitol providing only a slight advantage in detecting metabolites with lower signal (**Fig. 1e**). Furthermore, we tested the ability to detect two-fold changes in metabolites by performing serial dilution of the cellular inputs. The correlation of observed values of the diluted samples, to the predicted values that were based on the top concentration, was similar for both washes (**Fig. 1f**). Given similar performance with our platform, we chose mannitol for our subsequent experiments. Mannitol has been used to reduce the ionic matrix and its effect on electrospray ionization and enhance performance of other technologies, such as capillary electrophoresis[42,45–47], as an alternative to hypotonic methods[32,48].

Ultimately, our goal was to compare equal cellular inputs of differently treated T-cells, which is different from serial dilution, where sample matrix is halved artificially and could have unpredictable effects related to ion suppression[49,50]. Thus, as a control perturbation of metabolism, we substituted galactose for glucose in cell culture media, which is known to decrease glycolytic flux and force cells to respire[18,51–53] (**Fig. 1g**). We used 8.4 x 10^5 activated human T-cells per replicate, based on our serial dilution experiment. Lactate production was suppressed when cells were grown in the galactose-containing medium (**Fig. 1h**). The results of this experiment are displayed in **Table 1**. We detected higher levels of the Leloir pathway intermediates UDP-hexose and hexose-phosphate with galactose treatment. Aspartic acid was also elevated, consistent with recent reports that intracellular aspartic acid levels increase as a result of respiration in proliferating cells[54,55]. Glycolytic intermediates were higher in the glucose condition, as was UDP N-acetylglucosamine, which is reflective of higher available glucose pools for the hexosamine pathway[56]. Thus, the findings fit expectations based on the literature.

Compound	fold change glucose vs. galactose	p.value	FDR	pathway
UDP-hexose	-1.42	6.39×10^{-5}	7.46×10^{-04}	Leloir
Hexose-phosphate	-8.98	4.07×10^{-4}	3.36×10^{-03}	both
Fructose-1,6-bisphosphate	9.22	8.37×10^{-7}	2.34×10^{-05}	glycolysis
Glyceraldehyde-3-P	1437.38	9.12×10^{-4}	4.91×10^{-03}	glycolysis
Dihydroxyacetone-P	583.69	6.54×10^{-3}	2.41×10^{-02}	glycolysis
3-phosphoglycerate	2.75	4.90×10^{-4}	3.61×10^{-03}	glycolysis
Phosphoenolpyruvate	1.24	7.23×10^{-1}	8.04×10^{-01}	glycolysis
Pyruvate	-1.52	4.44×10^{-1}	5.92×10^{-01}	glycolysis
Lactate	44.66	2.41×10^{-6}	3.97×10^{-05}	glycolysis
UDP N-acetylglucosamine	16.26	1.46×10^{-6}	2.92×10^{-05}	misc
Aspartic Acid	-5.97	4.76×10^{-4}	3.61×10^{-03}	misc

Table 1. Intracellular metabolite level changes of activated human primary T-cells in culture medium containing Glucose vs. Galactose.
Summary of three experiments with each condition performed in triplicate.

CHAPTER 3

T-cell activation and checkpoint system

Having established the parameters needed to detect expected metabolic changes from a known nutrient restriction manoeuver in human primary T-cells, we were next interested in examining metabolic changes imposed by negative signaling through the programmed cell death 1 receptor (PDCD1/PD-1). There are several available options to activate T-cells in vitro. These include superantigen toxins, mitogens, phorbol esters, activating antibodies, and artificial antigen presentation[57,58]. Activating antibodies, immobilized to culture vessel surfaces or paramagnetic beads, have become popular due to their ease of use compared to cellular antigen presentation systems and improved functional outcomes compared to mitogens[58,59]. The optimization focus has been on maximal activation and expansion or maximal cytokine production, in part driven by adoptive cell transfer efforts[60,61], as higher numbers of transferred cells have correlated with better outcomes and minimum thresholds for transfer are commonly used[6,62]. There are reports of the use of such antibodies in conjunction with recombinant human PD-L1 peptide, but they differ in their recommendation of the delivery method of the inhibitory ligand[63–66]. None of these methods has used a cell-based antigen presentation system as a benchmark of physiologic activation.

We adapted a plate-based activation system[67] that used antibodies for artificial co-stimulation of T-cells through CD3 and CD28, and either Fc fragment of IgG as control or a recombinant human protein ligand of PD-1 conjugated to Fc (rhPD-L1.Fc) for concurrent T-cell inhibition (**Fig. 2a**). Treatment of peripheral blood mononuclear cells with a clinical-grade adoptive cell transfer expansion protocol[61], caused increased cell-surface expression of PD-1 (data not shown).

The conditions of this protocol favor expansion of T-cells over other peripheral blood mononuclear cells (PBMCs), but we also incorporated an immunomagnetic T-cell isolation step prior to treatment. After isolation on day 7, T-cells were placed in the treatment plates, as depicted in **Figure 2a**.

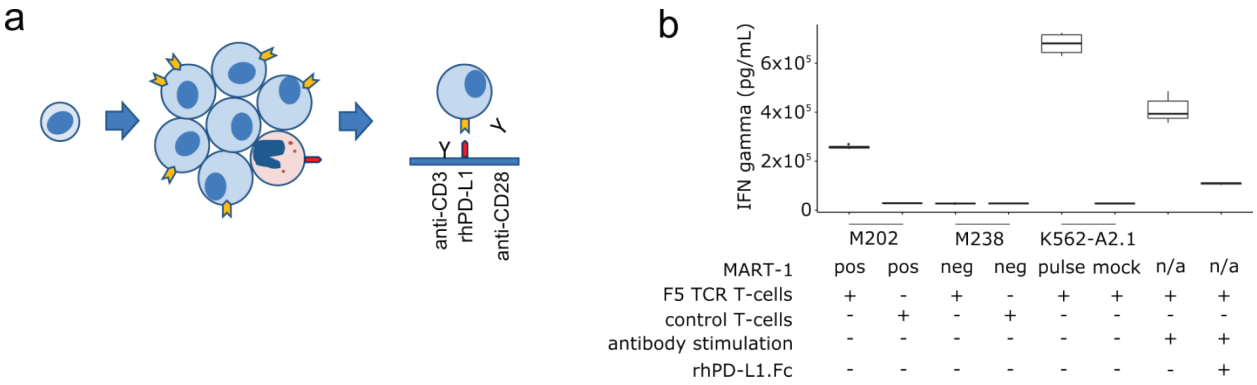

Figure 2. Recombinant human PD-L1 efficiently inhibits T-cells activated by antibody-based stimulation.

(a) Schematic representation of T-cell treatment prior to metabolite extraction. PBMC are expanded using a clinical grade adoptive cell transfer protocol that leads to upregulation of PD-1 receptor on the surface of T-cells. Isolated T-cells are then seeded in plates with anti-CD3 and anti-CD28 antibodies with or without recombinant human PD-L1 (rhPD-L1). **(b)** IFN gamma ELISA of 24 hour supernatants. T-cells bearing an exogenously expressed MART-1 specific T-cell receptor (F5 TCR) were co-cultured with M202 melanoma cells that present MART-1 via HLA-A2.1, M238 cells that do not, K562 cells with exogenous expression of HLA-A2.1 pulsed with MART-1_{26-35} peptide, or stimulated with anti-CD3 and anti-CD28 antibodies without target cells. Importantly, anti-CD3 and anti-CD28 antibody-based stimulation activates T cells to comparable levels as does cell-based melanoma antogen presentation.

To simulate known pathophysiology and ensure that the rhPD-L1.Fc could inhibit in-vitro antibody-based stimulation that was relevant to cell-based activation, we made use of transgenic T-cell receptor-bearing effector cells (F5 TCR) in co-culture with melanoma or K562 erythroleukemia cell lines presenting cognate MART-1 antigen[68]. We titrated antibody-based activation to produce similar levels of interferon gamma (IFNg) compared to cell-based

activation, and we demonstrated that the ligand effectively inhibited this response (**Fig. 2b**), thus generating a system to study immune activation and inhibition by PD-L1.

CHAPTER 4

PD-L1 checkpoint induced metabolic changes

With our newly established extraction method, we interrogated metabolic changes in T-cells caused by negative PD-L1:PD-1 axis signaling using liquid chromatography-mass spectrometry (LC-MS). After 72 hours of treatment, an overview of the 146 adequately measured intracellular metabolites of our 155 metabolite panel showed most to be decreased as a result of rhPD-L1.Fc treatment (**Fig. 3a**). The glycolysis pathway metabolites were significantly decreased compared to the Fc control (**Fig. 3b**) consistent with reports of a shift away from aerobic glycolysis[16,17]. Metabolic profiling of the culture medium showed that rhPD-L1.Fc-treated cells produced significantly less lactate and alanine in 24 hours and consumed less glucose, glutamine and serine (**Fig. 3c**), consistent with a less activated, less anabolic state, and a shift away from aerobic glycolysis and glutaminolysis[17,28]. Inhibited cells had higher levels of the pyrimidine nucleoside precursor aspartate and lower levels of nucleoside phosphates (**Fig. 3d**).

To further investigate these changes we performed [U-^{13}C] glucose tracer experiments. By analyzing the steady-state isotopomer distributions of metabolites, one can gain insight into relative pathway activities, particularly for non-linear pathways with multiple possible contributing pathways, such as the TCA cycle[69]. In the inhibited condition, we found fewer glucose derived 2-carbon units entering via pyruvate resulting in less citrate M2, suggesting an alternate source of acetyl-CoA (**Fig. 4a**). Less unlabeled a-ketoglutarate M0 suggested fewer unlabeled carbons from glutaminolysis. Succinate M0 fractional labeling was reversed, suggesting more unlabeled carbons entering at succinyl-CoA, possibly from the terminal 3-carbon units of odd chain fatty acids or branched chain amino acids (BCAA). We did not

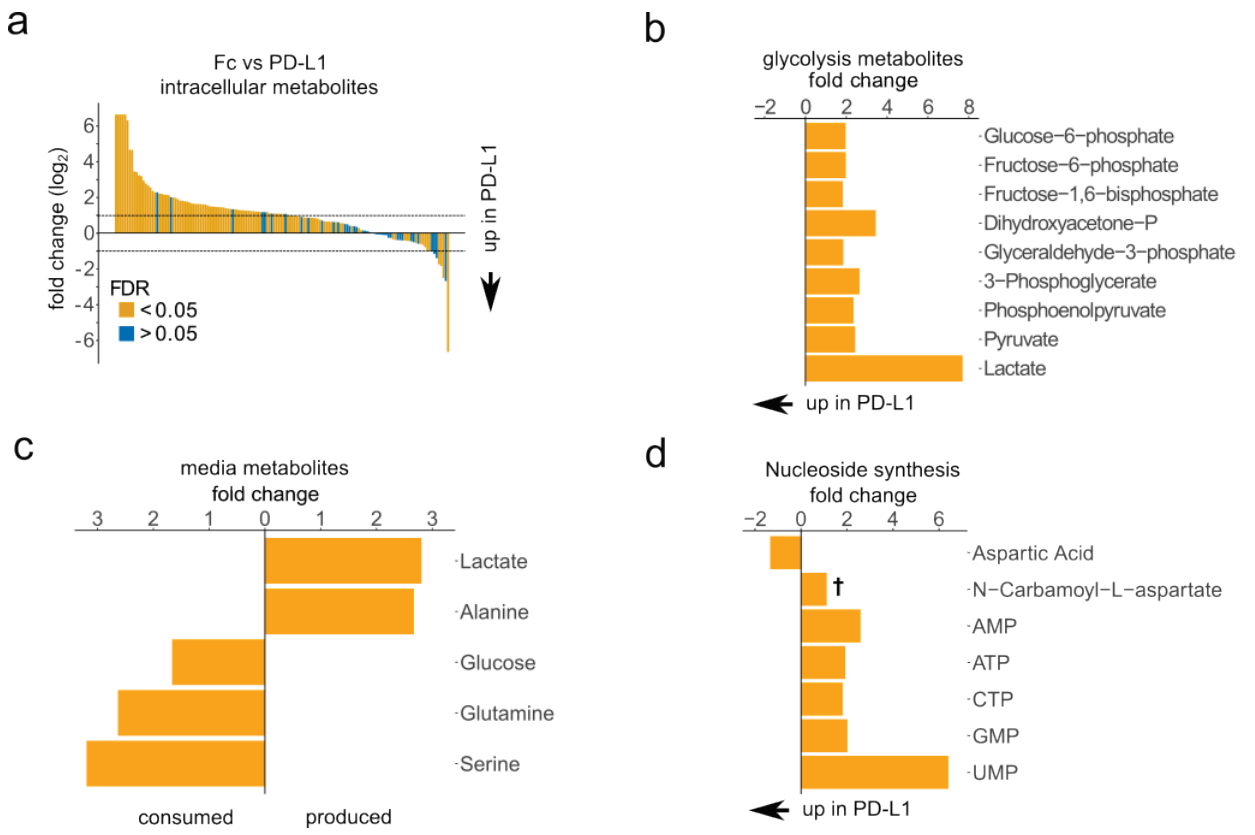

Figure 3. Relative levels of intracellular and supernatant metabolites in activated vs. PD-L1-inhibited T-cells.

(a) Overview of all profiled intracellular metabolites as measured by mass spectrometry. Positive values indicate higher levels in the activated condition (Fc). Dotted lines represent a two-fold change on the $\log_2$ scale. **(b)** Glycolysis pathway intracellular metabolites are higher in activated cells. **(c)** Compared to PD-L1 treated cells, more lactate and alanine are produced, and more glucose, glutamine and serine are consumed by activated T-cells. **(d)** Nucleoside phosphates are increased and aspartic acid levels are decreased in activated T-cells. FDR: false discovery rate. †: FDR > 0.05. All values represent four experiments with triplicates of each condition and have FDR < 0.05 unless indicated otherwise. Values are capped at 100-fold in panel **a**.

measure oxaloacetate directly, but we determined that aspartate was not consumed from the media in either condition and thus its labeling pattern was interpreted to be in equilibrium with oxaloacetate based on past studies[69]. Hence, higher aspartate M3 indicated pyruvate carboxylation, three labeled carbons coming from pyruvate and one unlabeled carbon from CO_2[69–71]. Despite similar levels of ribose-5-phosphate labeling (**Fig. 4b**) and higher total aspartic

acid labeling, there were significant decreases in UMP M5 and UMP M6-7, reflecting lack of incorporation of labeled carbons from ribose-5-P and aspartic acid respectively. This labeling pattern was apparent in the majority of the profiled nucleoside phosphates (data not shown). Taken as a whole, these changes suggest a switch from aerobic glycolysis and glutaminolysis to alternative contributing pathways, such as fatty acid beta oxidation and BCAA catabolism, and is consistent with a substantial reduction in the synthesis of nucleosides de novo (**Fig. 4c**).

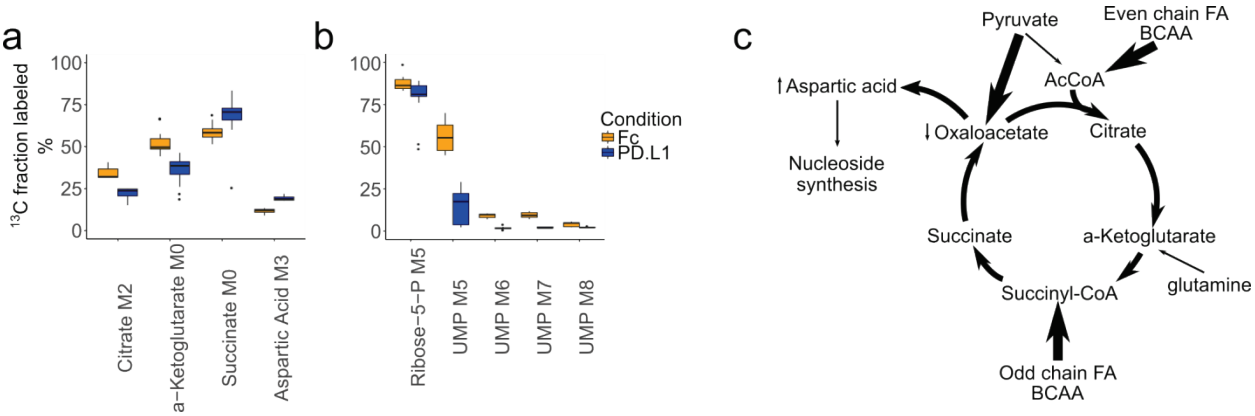

Figure 4. [U-^{13}C] glucose tracing shows differences in metabolite contribution to the TCA cycle and decreased nucleoside phosphate synthesis upon PD-L1 inhibition.

(a) Select isotopomers of TCA metabolites used to infer metabolite contributions to the TCA cycle, expressed as the percentage of all isotopomers detected for the respective compounds. M0: unlabeled. M2: Two heavy carbons from glucose. M3: Three heavy carbons from glucose. **(b)** Select isotopomers of uridine monophosphate and ribose-5-phosphate that represent the contribution of fully labeled ribose-5-phosphate (UMP M5) plus partially labeled aspartic acid (UMP M6-7). **(c)** Schematic of inferred relative metabolic pathway contributions to the TCA cycle in PD-L1 treated cells. Thick arrows represent more relative contribution of a pathway in the PD-L1 treated cells compared to the Fc control.

To our knowledge, a shutdown in nucleoside phosphate de novo biosynthesis as a result of PD-1 ligation has not been previously documented. De novo pyrimidine and purine biosynthesis is required for cell cycle progression and proliferation of activated T-cells[72]. We questioned whether this negative regulation could be an early event and a potential early metabolic checkpoint[15]. If so, we wondered whether circumventing the block in nucleoside phosphate

synthesis would rescue the proliferation defect that accompanies PD-L1:PD-1 axis signaling[73]. Thus, we assayed metabolites at an earlier 24 hour time-point. Our findings were again consistent with reduced glycolysis and glutaminolysis, but overall changes were more modest. Among relative level changes caused by rhPD-L1.Fc treatment with an FDR < 0.05, we found decreased ribose-5-P and UMP, and an increased pool of aspartic acid (**Fig. 5a**). A tracer experiment with [U-^{13}C] glucose showed that the inhibited cells incorporated less ^{13}C from ribose-5-P. At this early timepoint, the fold reduction was larger for pyrimidines than purines (**Fig. 5b**).

The mechanistic target of rapamycin complex 1 (mTORC1) has been shown to regulate nucleoside phosphate synthesis. The first committed step in pyrimidine synthesis is controlled by an activating phosphorylation of the trifunctional enzyme carbamoyl-phosphate synthetase 2, aspartate transcarbamylase, and dihydroorotase (CAD) by mTORC1[74]. Purine synthesis is induced by mTORC1 through transcriptional upregulation of genes, including methylenetetrahydrofolate dehydrogenase 2 (MTHFD2)[75]. By western blotting, we probed phosphorylation sites on downstream targets of mTORC1, including CAD, and found decreased activity with rhPD-L1 treatment (**Fig. 5c**). In certain cellular contexts, isolated deficiency of nucleoside phosphate synthesis can be rescued by providing substrates downstream of the level of the block, including nucleosides themselves[74–76]. Thus, we supplemented rhPD-L1-treated T-cells with a cocktail of nucleosides (cytidine, guanosine, uridine, adenosine, thymidine; Embryomax®, Millipore # ES-008-D) of varied concentration and measured the effect on cell number after 48 hours of treatment. We were not able to document a consistent dose-dependent rescue effect on cell number by assaying total DNA fluorescence, nor by reductive capacity (**Fig. 5d**).

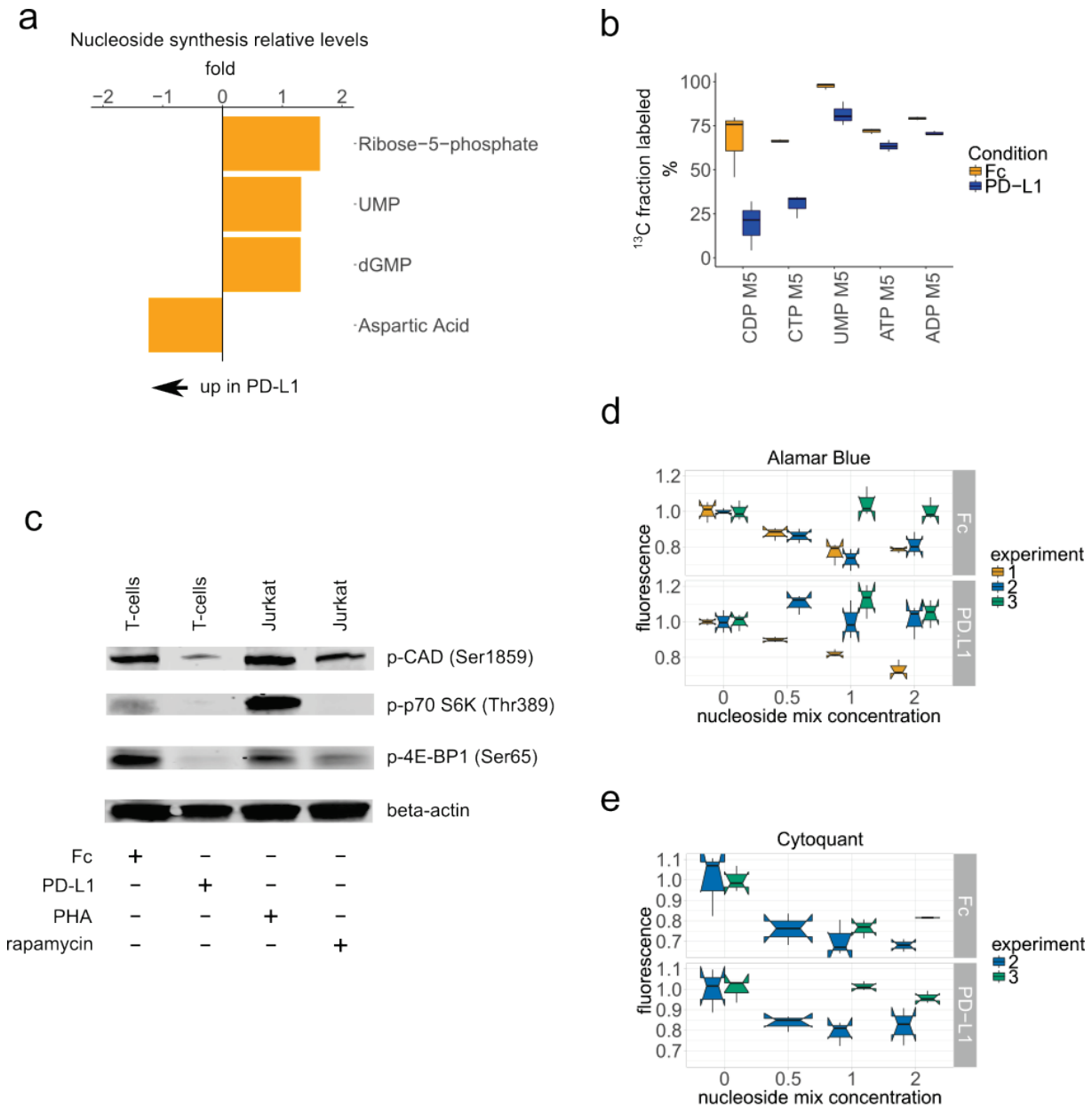

Figure 5. Nucleoside phosphate synthesis deficiency is an early event with PD-L1 inhibition, particularly for pyrimidines.

(a) Relative levels of nucleoside phosphates and aspartic acid at 24 hours of treatment. **(b)** Statistically significantly changing ^{13}C incorporation into nucleoside phosphates from [U-^{13}C] glucose. All measurements have a FDR<0.05 but the fold-reduction is larger for pyrimidines than for purines. **(c)** Western blot of phosphorylation status of mTORC1 targets. T-cells were treated for 48 hours as indicated. Jurkat cells were treated for 2 hours. PHA: phytohemagglutinin 5 µg/mL. Rapamycin dose: 20 nM. **(d)** Alamar blue resarufin fluorescence assay of Fc and PD-L1 treated T-cells with or without nucleoside cocktail supplementation for

48 hours. **(e)** DNA fluorescence assay of Fc and PD-L1 treated T-cells with or without nucleoside cocktail supplementation for 48 hours.

CHAPTER 5

Discussion

The use of a simple centrifugation-based extraction protocol specifically optimized for T-cells enabled us to measure relative level changes of metabolites and perform ^{13}C label tracing of metabolic pathways using 8.4 x 10^5 cells per replicate, a more than 35-fold reduction in cell input requirement compared to 3 x 10^7 cells used in previous studies[17,28]. Our data recapitulated what is known about mammalian cells forced to respire while growing with galactose as their carbon source[18,51–53]. We generated a system for studying T-cell activation and inhibition, and we were able to clearly demonstrate that PD-L1 treatment decreases glycolytic flux and glutaminolysis, in line with previous studies[16,17]. We extended what is known about PD-L1 induced metabolic reprogramming in human T-cells by giving a detailed picture of altered TCA cycle pathway contributions and demonstrating reduced de novo nucleoside phosphate synthesis.

To our knowledge, the negative effects of ammonium acetate on metabolite measurements have not previously been reported, whereas the poor yields with methanol wash solutions have[30,34,44]. The permeability of mammalian cells to ammonium salts of weak acids is known, given that they have been studied as cell-penetrating cryopreservation agents[77–79]. Thus, the swelling of cells with prolonged exposure could have been predicted. A study with primary focus on lipidomics in Jurkat cells came to the conclusion that ammonium acetate is appropriate for human mammalian non-adherent cell metabolomics[31]. A study using ammonium acetate as a wash solution for secondary ion mass spectrometry (SIMS) found no significant effect on viability, however the wash solution was “added and immediately removed” and optimization parameters would be different than for LC-MS experiments[80]. We found that 150 mM ammonium acetate is

not an isotonic solution, consistent with its ability to permeate cell membranes, and in our assay this led to more variable results. We were able to improve the consistency of our measurements by using mannitol (**Fig. 1c**). This highlights that in developing an extraction protocol, one needs to take into consideration many factors and to tailor the method to the particular application, while making sure to test prior reports for applicability and reproducibility in the new context.

It follows from above that our extraction protocol may have certain limitations if applied differently. In the case of SIMS imaging, washing with a sucrose solution left an interfering residue[80], and it is likely that mannitol would do the same. The most attractive property of ammonium salts of weak acids is their volatility. Osmotic effects are less drastic than with deionized water[80] (and data not shown) and the ions will evaporate with drying, thus eliminating ion suppression. Thus, ammonium salts possibly remain preferable to mannitol for very short exposure washes, such as with adherent cells. Even at ice-cold temperatures, certain very low abundance metabolites with high conversion rates can still be metabolized in the 4 min it takes to complete our wash and thus go undetected. For profiling of such metabolites, a fast filtration method may be necessary. Our metabolite profiling parameters allowed us to sufficiently demonstrate changes in cells forced to respire with galactose, or treated for 24-72 hours with rhPD-L1.Fc but adjustments may be required to profile more subtle phenotypes.

Treatment of activated T-cells with PD-L1 reduces aerobic glycolysis and glutaminolysis, and cells use beta oxidation of fatty acids as an alternative fuel source[16,17]. Our tracer experiments are consistent with more unlabeled acetyl groups entering the TCA cycle from fatty acid oxidation and the conversion of other substrates. This would be expected to inhibit the pyruvate dehydrogenase complex and it would explain why we see carboxylation of pyruvate to

oxaloacetate[70]. Our data does not corroborate that PD-1 signaling impairs branched chain amino acid oxidation[17]. We don't see the same changes in relative levels of these amino acids as previously reported. The contribution of odd chain fatty acids to succinyl-CoA is only the terminal 3 carbons of the chain, all others entering through acetyl-CoA. Thus, it is probable that the large influx of unlabeled carbons at succinyl-CoA represents other substrates, among which isoleucine and valine are candidates. Labeled BCAA studies would be necessary to confirm this. We found higher relative levels of aspartate in PD-L1 treated cells, but relative levels of a metabolite in isolation are hard to interpret, as either increased production or reduced consumption could be the cause. Distinguishing between the two is difficult without the appropriate labeled tracer study[69]. Two groups have shown that increased function of the electron transport chain results in higher production of aspartate[54,55]. However, although PD-L1-treated cells rely more on fatty acid beta oxidation, it has been shown that their net basal oxygen consumption rate is decreased[17]. We see a decrease in de novo nucleoside phosphate biosynthesis, making it more compelling to hypothesize that less aspartate is being consumed to produce pyrimidines.

It was reported that mTORC1 controls pyrimidine biosynthesis via signaling-based mechanisms involving phosphorylation-based activation of CAD[74]. mTORC1 also controls purine biosynthesis, but typically on a longer time-frame through transcriptional regulation[75]. Nucleoside phosphate de novo synthesis is a requirement for T-cells to proliferate[72] and thus represents a metabolic checkpoint. We found that decreased de novo synthesis of nucleoside phosphates is present as early as 24 hours during treatment, is more pronounced in pyrimidines at this time point, but is substantially seen for both pyrimidines and purines by 72 hours. This kinetic pattern is consistent with the typically quicker signaling-based regulation of pyrimidine

synthesis, in comparison to the transcription-based regulation of purine synthesis summarized above. We also observed that phosphorylation of mTORC1 targets was decreased. In our experiments, we were not able to rescue proliferation in PD-L1 treated cells by providing exogenous nucleosides. It is possible that a different dosing scheme with an optimized balance of each nucleoside may have resulted in an observable rescue. But even if the requirements of import and phosphorylation of nucleosides were met, an inability to rescue would not be entirely unexpected, as mTOR controls many other cellular processes[81]. Additionally, PD-L1:PD-1 negative signaling is known to engage cell cycle checkpoints[82–84] that are attributed to non-metabolic mechanisms.

In conclusion, we have developed an easily transferable and low-input metabolite extraction protocol for human T-cells and have used it to show that in addition to its known metabolic effects, PD-L1 inhibits nucleoside phosphate de novo biosynthesis. Our data demonstrate that multiple metabolite levels are decreased with inhibitory signaling, suggesting broad metabolic regulation. This would be expected with downregulation of mTOR signaling, often referred to as a "master regulator of metabolism". It would also suggest that correcting isolated metabolic pathway defects may not be sufficient to restore T-cell function without significant concurrent manipulation of cell signaling, as we saw with our nucleoside supplementation experiment. The same does not necessarily hold true for augmenting immunotherapy. A recent metabolomics study profiled changes of activated naïve cells and showed a role for arginine metabolism in enhancing T-cell survival and anti-tumor activity[85] and a follow up study by another group showed that arginine supplementation enhanced the efficacy of anti-PD-L1 treatment in a mouse model of osteosarcoma[86]. Thus, further mining of our existing metabolomics data combined with other omics data[85] would be promising to generate hypotheses regarding beneficial

metabolic manoeuvers that could be tested with adoptive cell transfer models. Our activation system can be easily adapted to interrogate the metabolic effects of drugs, cytokines, stimulatory and inhibiting interactions that may be of interest to individual immunometabolism labs. It is interesting to speculate what we can be taught about T-cell memory with our existing data and a combined omics approach, given that oxygen consumption profiles of PD-L1 treated human T-cells and IL-15 memory-polarized murine cells both display an increase in spare respiratory capacity[17,22] and that PD-L1 mediated exhaustion can be reversed, at least to a certain extent, with checkpoint inhibition therapy[87].

CHAPTER 6

Methods

Cell lines and culture.

Human peripheral blood mononuclear cells, Jurkat cells, M202 and M238 melanoma cells were grown in RPMI 1640 with glutamine supplemented with 10% fetal calf serum and 1% SPF antibiotic. Immortalized mouse embryonic fibroblasts were cultured in DMEM. Peripheral blood mononuclear cells (PBMCs), Jurkat cells and melanoma cells were provided by Dr Antoni Ribas. MEFs were immortalized in our lab as previously described[88].

Timed exposure to wash solutions - Jurkat cell morphology.

Jurkat T-cell leukemia cells were seeded into poly-D-Lysine coated 96-well plates at 2 x 10^5 cells per well in cell culture medium and centrifuged at 30 x G-force for 1 minute with the brake off. The plate was placed on a Nikon eclipse Ti microscope stage. One well at a time, the cell culture medium was aspirated and replaced with the indicated ice-cold wash solutions. Images were acquired at the indicated times.

Wash solution time-course with adherent cells for metabolomics.

Spontaneously immortalized mouse embryonic fibroblasts were seeded in triplicate at 2.5 x 10^5 cells per 9 cm^2 and incubated overnight to allow for attachment. The culture medium was aspirated one replicate at a time and washed with either ice-cold 150 mM ammonium acetate aqueous solution or 0.9% (w/v) NaCl solution. The wash solution was aspirated either immediately, at 20 seconds, or at 60 seconds. The plate was placed on ice. Metabolites were extracted directly from the plate with 1 mL ice-cold 80% (v/v) methanol/H_2O. The cells were

scraped and the content of the plate transferred to a 1.5 mL plastic disposable centrifuge tube and placed first on dry ice and then into a -80° freezer until further processing.

Serial dilution of Jurkat cells and centrifugation-based extraction.

Jurkat cells were serially two-fold diluted to give 2 x 10^6, 1 x 10^6, and 0.5 x 10^6 cells per replicate. The cells were separated from culture medium by centrifugation at 500 x G-force for 4 min followed by aspiration. Mannitol or NaCl ice cold solutions of 1 mL volume were added and followed by a second centrifugation using the same parameters at 4° C. After aspirating the wash solution the cells were immediately extracted using 250 µL ice-cold methanol, followed by 250 µL diH_2O, and then 250 µL chloroform, vortexing briefly in between steps. The mixture was centrifuged at top speed for 5 min at 4° C and the upper aqueous phase was collected into a glass chromatography vial and stored at -80° C until further processing as described below for T-cell metabolomics.

Carbon source experiments.

Glucose-free RPMI 1640 (ThermoFisher #11879020) was supplemented with 10 mM glucose or galactose, 10% dialyzed fetal calf serum and 1% SPF. Cells were seeded in activating conditions in 12-well plates at 8.4 x 10^5 cells per 500 µL culture medium in triplicate for each carbon source. After 24 hours, media was collected and intracellular metabolites extracted as per the T-cell metabolite extraction protocol below.

T-cell directed expansion of peripheral blood mononuclear cells (PBMCs).

Human PBMCs were expanded toward the T-cell lineage as previously described[61] with modifications. Cryopreserved cells at 1 x 10^7 cells/mL were thawed and diluted in RPMI containing 10% fetal calf serum and 1% penicillin, streptomycin and amphotericin by adding

1mL cells to 5mL warm media, followed by centrifugation at 500 xG-force for 4 min and replacement of supernatant with 1mL fresh medium containing DNAse 227 U/mL for 45 min at 37° C without disturbing the pellet. The cells were resuspended with 9 mL medium and a 10 µL aliquot was counted before another round of centrifugation and placement in fresh medium in tissue culture flasks at 7 x 10^5 cells/mL. The cells were incubated for 48 hours with 50 ng/mL OKT3 anti-CD3 antibody in solution (OKT3, Miltenyi Biotec, Auburn, CA) and 300 IU/mL IL-2. The medium was then replaced with 300 IU/mL IL-2-containing medium for the duration of expansion. Medium acidity was monitored and fresh medium added to maintain a concentration of 7 x 10^5 cells/mL approximately every two days.

T-cell activation and treatment with PD-L1

Treatment plates were coated at 4° C overnight with 1 µg/mL anti-CD3 antibody (BD biosciences 555329) and 1.5 µM human IgG Fc fragment (Jackson Immunoresearch #009-000-008) or 1.5 µM rhPD-L1.Fc (Sino Biological #10084-H02H) in 1.2 mL PBS per well of a 12-well non-tissue culture treated plate (Corning #351143). The antibody-coated plate was then washed twice with 2 mL PBS and blocked for 1 hour at room temperature with 1.5 mL human serum albumin 2.5% in PBS, followed by two more washes with PBS. T-cells expanded for 7 days were isolated by use of an immunomagnetic negative enrichment kit (ThermoFisher #11344D) and seeded in triplicate wells at 8.4 x 10^5cells in 1.2 mL glucose-free RPMI (ThermoFisher #11879020) treatment medium supplemented with 10 mM [U-^{13}C] glucose (Cambridge Isotope Laboratories #CLM-1396-PK), 10% dialyzed fetal calf serum, 1% SPF, and 1 µg/mL anti-CD28 antibody (BD biosciences # 555725). For 72 hour treatments, the treatment medium was refreshed 24 hours prior to harvest.

T-cell metabolite extraction protocol

Treated T-cells were harvested into microcentrifuge tubes and centrifuged at 500 x G-force for 4 min. The medium was collected into separate tubes and placed on dry ice and then into -80° C until further processing. Ice-cold 5.4% mannitol wash solution was added, 1 mL to each pellet and centrifuged with the same parameters at 4° C. All subsequent steps are performed on ice with all solutions ice-cold. The wash solution was removed and 250 µL methanol added, then 250 µL water, and finally 250 µL chloroform, vortexing briefly in between steps. The mixture was centrifuged at 16,000 x G-force for 5 min. The top polar phase was collected into glass chromatography vials and stored at -80° C until further processing. The tube was tilted carefully to expose the non-polar phase which was collected separately, but not included in this analysis. The interphase was retained for later protein quantitation with a BCA assay kit (ThermoFisher #23225) per manufacturer microplate protocol. The polar phase, 20 µL of the supernatants, and three mock extracted controls per run (polar phase of extraction mixture without cells) were evaporated with an EZ2 Elite centrifugal evaporator for 80 min on HPLC setting with 30° C maximum temperature. The samples were block randomized and stored at -80° C prior to recovery and submission to mass spectrometry.

Liquid chromatography and mass spectrometry

Metabolites were recovered in 50 µL 70% ACN and 5 µL of this solution used for mass spectrometer-based analysis performed on a Q Exactive (Thermo Scientific) coupled to an UltiMate 3000RSLC (Thermo Scientific) UHPLC system. Mobile phase A was 5 mM NH4AcO, pH 9.9, B was ACN, and the separation achieved on a Luna 3u NH2 100A (150 × 2.0 mm) (Phenomenex) column. The flow was kept at 200 µL/min, and the gradient was from 15% A to

95% A in 18 min, followed by an isocratic step for 9 min and re-equilibration for 7 min. Metabolites we detected and relatively quantified as area under the curve (AUC) based on retention time and accurate mass (≤ 3 p.p.m.) using TraceFinder 3.3 (Thermo Scientific) software.

Co-culture of transgenic T-cells with melanoma and K562 targets.

Production of transgenic MART-1 specific TCR bearing T-cells was previously described[68]. Twenty-four hour IFNg secretion into the supernatant was assayed by ELISA (ThermoFisher #88-7316-77). Antibody stimulation is described in the T-cell activation section.

Western blotting

Primary antibodies used were Phospho-CAD (Ser1859) Antibody #12662, Phospho-p70 S6 Kinase (Thr389) (108D2) Rabbit mAb #9234, Phospho-4E-BP1 (Ser65) (174A9) Rabbit mAb #9456, and β-Actin (D6A8) Rabbit mAb #8457 from Cell Signaling.

REFERENCES

1. Gotwals, P. *et al.* Prospects for combining targeted and conventional cancer therapy with immunotherapy. *Nat Rev Cancer* **17,** 286–301 (2017).
2. Zanetti, M. Tapping CD4 T Cells for Cancer Immunotherapy: The Choice of Personalized Genomics. *The Journal of Immunology* **194,** 2049–2056 (2015).
3. Kantoff, P. W. *et al.* Sipuleucel-T immunotherapy for castration-resistant prostate cancer. *N. Engl. J. Med.* **363,** 411–422 (2010).
4. Kantarjian, H. *et al.* Blinatumomab versus Chemotherapy for Advanced Acute Lymphoblastic Leukemia. *N. Engl. J. Med.* **376,** 836–847 (2017).
5. Kochenderfer, J. N. *et al.* Chemotherapy-refractory diffuse large B-cell lymphoma and indolent B-cell malignancies can be effectively treated with autologous T cells expressing an anti-CD19 chimeric antigen receptor. *J. Clin. Oncol.* **33,** 540–549 (2015).
6. Rosenberg, S. A. *et al.* Durable complete responses in heavily pretreated patients with metastatic melanoma using T-cell transfer immunotherapy. *Clin. Cancer Res.* **17,** 4550–4557 (2011).
7. Lee, D. W. *et al.* T cells expressing CD19 chimeric antigen receptors for acute lymphoblastic leukaemia in children and young adults: a phase 1 dose-escalation trial. *Lancet* **385,** 517–528 (2015).
8. Besser, M. J. *et al.* Adoptive transfer of tumor-infiltrating lymphocytes in patients with metastatic melanoma: intent-to-treat analysis and efficacy after failure to prior immunotherapies. *Clin. Cancer Res.* **19,** 4792–4800 (2013).
9. Sharma, P. & Allison, J. P. The future of immune checkpoint therapy. *Science* **348,** 56–61 (2015).

10. Topalian, S. L., Drake, C. G. & Pardoll, D. M. Immune checkpoint blockade: a common denominator approach to cancer therapy. *Cancer Cell* **27,** 450–461 (2015).
11. Tumeh, P. C. *et al.* PD-1 blockade induces responses by inhibiting adaptive immune resistance. *Nature* **515,** 568–571 (2014).
12. Shin, D. S. *et al.* Primary Resistance to PD-1 Blockade Mediated by JAK1/2 Mutations. *Cancer Discov* CD-16-1223 (2016). doi:10.1158/2159-8290.CD-16-1223
13. Zaretsky, J. M. *et al.* Mutations Associated with Acquired Resistance to PD-1 Blockade in Melanoma. *N. Engl. J. Med.* **375,** 819–829 (2016).
14. Odorizzi, P. M., Pauken, K. E., Paley, M. A., Sharpe, A. & Wherry, E. J. Genetic absence of PD-1 promotes accumulation of terminally differentiated exhausted CD8+ T cells. *J. Exp. Med.* **212,** 1125–1137 (2015).
15. Wang, R. & Green, D. R. Metabolic checkpoints in activated T cells. *Nat Immunol* **13,** 907–915 (2012).
16. Parry, R. V. *et al.* CTLA-4 and PD-1 Receptors Inhibit T-Cell Activation by Distinct Mechanisms. *Mol Cell Biol* **25,** 9543–9553 (2005).
17. Patsoukis, N. *et al.* PD-1 alters T-cell metabolic reprogramming by inhibiting glycolysis and promoting lipolysis and fatty acid oxidation. *Nat Commun* **6,** (2015).
18. Chang, C.-H. *et al.* Posttranscriptional Control of T Cell Effector Function by Aerobic Glycolysis. *Cell* **153,** 1239–1251 (2013).
19. Chang, C.-H. *et al.* Metabolic Competition in the Tumor Microenvironment Is a Driver of Cancer Progression. *Cell* **162,** 1229–1241 (2015).
20. Ho, P.-C. *et al.* Phosphoenolpyruvate Is a Metabolic Checkpoint of Anti-tumor T Cell Responses. *Cell* **162,** 1217–1228 (2015).

21. Sukumar, M. *et al.* Inhibiting glycolytic metabolism enhances CD8+ T cell memory and antitumor function. *J. Clin. Invest.* **123,** 4479–4488 (2013).
22. van der Windt, G. J. W. *et al.* Mitochondrial respiratory capacity is a critical regulator of CD8+ T cell memory development. *Immunity* **36,** 68–78 (2012).
23. Kawalekar, O. U. *et al.* Distinct Signaling of Coreceptors Regulates Specific Metabolism Pathways and Impacts Memory Development in CAR T Cells. *Immunity* **44,** 380–390 (2016).
24. Macintyre, A. N. & Rathmell, J. C. Activated lymphocytes as a metabolic model for carcinogenesis. *Cancer Metab* **1,** 5 (2013).
25. Patti, G. J., Yanes, O. & Siuzdak, G. Innovation: Metabolomics: the apogee of the omics trilogy. *Nature Reviews Molecular Cell Biology* **13,** 263–269 (2012).
26. Dang, L. *et al.* Cancer-associated IDH1 mutations produce 2-hydroxyglutarate. *Nature* **462,** 739–744 (2009).
27. Lunt, S. Y. *et al.* Pyruvate Kinase Isoform Expression Alters Nucleotide Synthesis to Impact Cell Proliferation. *Molecular Cell* **57,** 95–107 (2015).
28. Wang, R. *et al.* The Transcription Factor Myc Controls Metabolic Reprogramming upon T Lymphocyte Activation. *Immunity* **35,** 871–882 (2011).
29. Buck, M. D. *et al.* Mitochondrial Dynamics Controls T Cell Fate through Metabolic Programming. *Cell* (2016). doi:10.1016/j.cell.2016.05.035
30. Dietmair, S., Timmins, N. E., Gray, P. P., Nielsen, L. K. & Krömer, J. O. Towards quantitative metabolomics of mammalian cells: Development of a metabolite extraction protocol. *Analytical Biochemistry* **404,** 155–164 (2010).
31. Ulmer, C. Z., Yost, R. A., Chen, J., Mathews, C. E. & Garrett, T. J. Liquid Chromatography-Mass Spectrometry Metabolic and Lipidomic Sample Preparation Workflow for Suspension-

Cultured Mammalian Cells using Jurkat T lymphocyte Cells. *J Proteomics Bioinform* **8,** 126–132 (2015).

32. Lapainis, T., Rubakhin, S. S. & Sweedler, J. V. Capillary Electrophoresis with Electrospray Ionization Mass Spectrometric Detection for Single Cell Metabolomics. *Anal Chem* **81,** 5858–5864 (2009).
33. Sellick, C. A., Hansen, R., Stephens, G. M., Goodacre, R. & Dickson, A. J. Metabolite extraction from suspension-cultured mammalian cells for global metabolite profiling. *Nat. Protocols* **6,** 1241–1249 (2011).
34. Kronthaler, J., Gstraunthaler, G. & Heel, C. Optimizing high-throughput metabolomic biomarker screening: a study of quenching solutions to freeze intracellular metabolism in CHO cells. *OMICS* **16,** 90–97 (2012).
35. Volmer, M., Gettmann, J., Scholz, S., Büntemeyer, H. & Noll, T. A method for metabolomic sampling of suspended animal cells using fast filtration. *BMC Proc* **5,** P93 (2011).
36. Bordag, N. *et al.* Fast Filtration of Bacterial or Mammalian Suspension Cell Cultures for Optimal Metabolomics Results. *PLOS ONE* **11,** e0159389 (2016).
37. Pearce, E. L., Poffenberger, M. C., Chang, C.-H. & Jones, R. G. Fueling Immunity: Insights into Metabolism and Lymphocyte Function. *Science* **342,** 1242454 (2013).
38. Ghesquière, B., Wong, B. W., Kuchnio, A. & Carmeliet, P. Metabolism of stromal and immune cells in health and disease. *Nature* **511,** 167–176 (2014).
39. Hernández Bort, J. A. *et al.* Reduced quenching and extraction time for mammalian cells using filtration and syringe extraction. *Journal of Biotechnology* **182–183,** 97–103 (2014).
40. McCloskey, D., Utrilla, J., Naviaux, R. K., Palsson, B. O. & Feist, A. M. Fast Swinnex filtration (FSF): a fast and robust sampling and extraction method suitable for metabolomics

analysis of cultures grown in complex media. *Metabolomics* (2014). doi:10.1007/s11306-014-0686-2

41. Rabinowitz, J. D. & Kimball, E. Acidic Acetonitrile for Cellular Metabolome Extraction from Escherichia coli. *Anal. Chem.* **79,** 6167–6173 (2007).
42. Miwa, H. Leukemia cells demonstrate a different metabolic perturbation provoked by 2-deoxyglucose. *Oncology Reports* (2013). doi:10.3892/or.2013.2299
43. Lorenz, M. A., Burant, C. F. & Kennedy, R. T. Reducing Time and Increasing Sensitivity in Sample Preparation for Adherent Mammalian Cell Metabolomics. *Anal Chem* **83,** 3406–3414 (2011).
44. Bolten, C. J., Kiefer, P., Letisse, F., Portais, J.-C. & Wittmann, C. Sampling for metabolome analysis of microorganisms. *Anal. Chem.* **79,** 3843–3849 (2007).
45. Kim, D. *et al.* SHMT2 drives glioma cell survival in ischaemia but imposes a dependence on glycine clearance. *Nature* **520,** 363–367 (2015).
46. Nishikawa, K. *et al.* DNA methyltransferase 3a regulates osteoclast differentiation by coupling to an S-adenosylmethionine-producing metabolic pathway. *Nat. Med.* **21,** 281–287 (2015).
47. Hirayama, A. & Soga, T. in *Capillary Electrophoresis–Mass Spectrometry (CE-MS)* (ed. Jong, G. de) 293–314 (Wiley-VCH Verlag GmbH & Co. KGaA, 2016). doi:10.1002/9783527693801.ch10
48. Miao, H., Rubakhin, S. S., Scanlan, C. R., Wang, L. & Sweedler, J. V. d-Aspartate as a putative cell–cell signaling molecule in the Aplysia californica central nervous system. *Journal of Neurochemistry* **97,** 595–606 (2006).

49. Annesley, T. M. Ion Suppression in Mass Spectrometry. *Clinical Chemistry* **49,** 1041–1044 (2003).

50. Tohge, T. *et al.* From Models to Crop Species: Caveats and Solutions for Translational Metabolomics. *Front Plant Sci* **2,** (2011).

51. Robinson, B. H. in *Methods in Enzymology* (ed. Giuseppe M. Attardi, A. C.) **264,** 454–464 (Academic Press, 1996).

52. Wilkens, C. A., Altamirano, C. & Gerdtzen, Z. P. Comparative metabolic analysis of lactate for CHO cells in glucose and galactose. *Biotechnol Bioproc E* **16,** 714–724 (2011).

53. Haverkorn van Rijsewijk, B. R. B., Nanchen, A., Nallet, S., Kleijn, R. J. & Sauer, U. Large-scale 13C-flux analysis reveals distinct transcriptional control of respiratory and fermentative metabolism in Escherichia coli. *Mol Syst Biol* **7,** 477 (2011).

54. Sullivan, L. B. *et al.* Supporting Aspartate Biosynthesis Is an Essential Function of Respiration in Proliferating Cells. *Cell* **162,** 552–563 (2015).

55. Birsoy, K. *et al.* An Essential Role of the Mitochondrial Electron Transport Chain in Cell Proliferation Is to Enable Aspartate Synthesis. *Cell* **162,** 540–551 (2015).

56. Wellen, K. E. *et al.* The hexosamine biosynthetic pathway couples growth factor-induced glutamine uptake to glucose metabolism. *Genes Dev* **24,** 2784–2799 (2010).

57. Muul, L. M. *et al.* Measurement of proliferative responses of cultured lymphocytes. *Curr Protoc Immunol* **Chapter 7,** Unit7.10 (2011).

58. Kim, J. V., Latouche, J.-B., Rivière, I. & Sadelain, M. The ABCs of artificial antigen presentation. *Nat Biotech* **22,** 403–410 (2004).

59. Functional impairment of human T-lymphocytes following PHA-induced expansion and retroviral transduction: implications for gene therapy. *, Published online: 03 October 2002; | doi:10.1038/sj.gt.3301807* **9,** (2002).

60. Trickett, A. & Kwan, Y. L. T cell stimulation and expansion using anti-CD3/CD28 beads. *Journal of Immunological Methods* **275,** 251–255 (2003).

61. Tumeh, P. C. *et al.* The impact of ex vivo clinical grade activation protocols on human T-cell phenotype and function for the generation of genetically modified cells for adoptive cell transfer therapy. *J. Immunother.* **33,** 759–768 (2010).

62. Weber, J. *et al.* White paper on adoptive cell therapy for cancer with tumor-infiltrating lymphocytes: a report of the CTEP subcommittee on adoptive cell therapy. *Clin. Cancer Res.* **17,** 1664–1673 (2011).

63. Brusa, D. *et al.* The PD-1/PD-L1 axis contributes to T-cell dysfunction in chronic lymphocytic leukemia. *Haematologica* **98,** 953–963 (2013).

64. Carter, L. L. *et al.* PD-1:PD-L inhibitory pathway affects both CD4+ and CD8+ T cells and is overcome by IL-2. *European Journal of Immunology* **32,** 634–643 (2002).

65. Freeman, G. J. *et al.* Engagement of the Pd-1 Immunoinhibitory Receptor by a Novel B7 Family Member Leads to Negative Regulation of Lymphocyte Activation. *J Exp Med* **192,** 1027–1034 (2000).

66. Bennett, F. *et al.* Program death-1 engagement upon TCR activation has distinct effects on costimulation and cytokine-driven proliferation: attenuation of ICOS, IL-4, and IL-21, but not CD28, IL-7, and IL-15 responses. *J. Immunol.* **170,** 711–718 (2003).

67. Atefi, M. *et al.* Effects of MAPK and PI3K Pathways on PD-L1 Expression in Melanoma. *Clin Cancer Res* **20,** 3446–3457 (2014).

68. Chodon, T. *et al.* Adoptive transfer of MART-1 T cell receptor transgenic lymphocytes and dendritic cell vaccination in patients with metastatic melanoma. *Clin Cancer Res* **20,** 2457–2465 (2014).

69. Buescher, J. M. *et al.* A roadmap for interpreting 13C metabolite labeling patterns from cells. *Curr Opin Biotechnol* **34,** 189–201 (2015).

70. Sugden, M. C. & Holness, M. J. The pyruvate carboxylase-pyruvate dehydrogenase axis in islet pyruvate metabolism: Going round in circles? *Islets* **3,** 302–319 (2011).

71. Divakaruni, A. S. *et al.* Inhibition of the mitochondrial pyruvate carrier protects from excitotoxic neuronal death. *J Cell Biol* jcb.201612067 (2017). doi:10.1083/jcb.201612067

72. Quéméneur, L. *et al.* Differential control of cell cycle, proliferation, and survival of primary T lymphocytes by purine and pyrimidine nucleotides. *J. Immunol.* **170,** 4986–4995 (2003).

73. Wei, F. *et al.* Strength of PD-1 signaling differentially affects T-cell effector functions. *PNAS* (2013). doi:10.1073/pnas.1305394110

74. Ben-Sahra, I., Howell, J. J., Asara, J. M. & Manning, B. D. Stimulation of de novo pyrimidine synthesis by growth signaling through mTOR and S6K1. *Science* **339,** 1323–1328 (2013).

75. Ben-Sahra, I., Hoxhaj, G., Ricoult, S. J. H., Asara, J. M. & Manning, B. D. mTORC1 induces purine synthesis through control of the mitochondrial tetrahydrofolate cycle. *Science* **351,** 728–733 (2016).

76. Patel, D. *et al.* Aspartate Rescues S-phase Arrest Caused by Suppression of Glutamine Utilization in KRas-driven Cancer Cells. *J. Biol. Chem.* **291,** 9322–9329 (2016).

77. Jacobs, M. H. & Stewart, D. R. The distribution of penetrating ammonium salts between cells and their surroundings. *J. Cell. Comp. Physiol.* **7,** 351–365 (1936).

78. Jacobs, M. H. Some Aspects of Cell Permeability to Weak Electrolytes. *Cold Spring Harb Symp Quant Biol* **8,** 30–39 (1940).

79. Sibinga, C. S., Das, P. C. & Meryman, H. T. *Cryopreservation and low temperature biology in blood transfusion*. (Springer Science & Business Media, 1990).

80. Berman, E. S. F. *et al.* Preparation of single cells for imaging/profiling mass spectrometry. *J. Am. Soc. Mass Spectrom.* **19,** 1230–1236 (2008).

81. Ben-Sahra, I. & Manning, B. D. mTORC1 signaling and the metabolic control of cell growth. *Curr. Opin. Cell Biol.* **45,** 72–82 (2017).

82. Brown, J., Patsoukis, N. & Boussiotis, V. A. PD-1 Signals Inhibit Cell Cycle Progression by Mediating Upregulation of Both KIP and INK Family of Cdk Inhibitors. *Blood* **116,** 585–585 (2010).

83. Patsoukis, N., Sari, D. & Boussiotis, V. A. PD-1 inhibits T cell proliferation by upregulating p27 and p15 and suppressing Cdc25A. *Cell Cycle* **11,** 4305–4309 (2012).

84. Patsoukis, N. *et al.* Selective effects of PD-1 on Akt and Ras pathways regulate molecular components of the cell cycle and inhibit T cell proliferation. *Sci Signal* **5,** ra46 (2012).

85. Geiger, R. *et al.* L-Arginine Modulates T Cell Metabolism and Enhances Survival and Anti-tumor Activity. *Cell* **167,** 829–842.e13 (2016).

86. He, X., Lin, H., Yuan, L. & Li, B. Combination therapy with L-arginine and α-PD-L1 antibody boosts immune response against osteosarcoma in immunocompetent mice. *Cancer Biol. Ther.* **18,** 94–100 (2017).

87. Pauken, K. E. & Wherry, E. J. Overcoming T cell exhaustion in infection and cancer. *Trends in Immunology* **36,** 265–276 (2015).

88. Graham, N. A. *et al.* Recurrent patterns of DNA copy number alterations in tumors reflect metabolic selection pressures. *Mol. Syst. Biol.* **13,** 914 (2017).